Paper No.
353

CORROSION 93
The NACE Annual Conference and Corrosion Show

CORROSION MEASUREMENT TECHNIQUES FOR STEEL IN CONCRETE

Alberto A. Sagüés
Department of Civil Engineering and Mechanics
University of South Florida
Tampa, Florida 33620

ABSTRACT

The present development of techniques for characterizing the extent of corrosion of reinforcing steel bars in concrete is reviewed. These methods include non-electrochemical test techniques such as visual inspection, soundings, direct examination, and electrical resistance. Electrochemical test methods involve observational measurements such as potential and resistivity surveys, macrocell current measurements, and electrochemical noise. Electrochemical polarization methods reviewed include large signal scans, polarization resistance, pulse techniques, and electrochemical impedance spectroscopy. Special attention is given to the effect of factors that complicate the polarization response of steel in concrete and affect the accuracy of corrosion rate measurements.

Key Words: Corrosion, steel, concrete, rebar, polarization, macrocell, resistivity, impedance, guard electrode.

INTRODUCTION

The Concrete Environment

Reinforcing steel bars (rebars) are placed in concrete to provide resistance to tensile stresses. In new concrete without contamination, the alkaline surroundings of the rebar surface cause it to be passive. The dissolution of metal proceeds at a very low rate. However, local depassivation may take place, for example, due to the penetration of chloride ions through the concrete cover from the external environment, or if the pH of the concrete pore liquids is reduced by interaction with atmospheric carbon dioxide [1]. In such cases, active corrosion of the reinforcing steel may begin. The corrosion products usually occupy a larger volume than that of the steel [2]. That causes the development of tensile stresses, which result in cracking of the

concrete. After cracking is initiated, further access from the corrosive environment to the steel surface can take place. Additional degradation of the structure may thus result. This form of corrosion has received extensive attention in recent years, as it threatens the integrity of the transportation and building infrastructure worldwide [1,3,4]. Methods for the detection and measurement of corrosion of steel in concrete have also received extensive attention. The material in contact with the imbedded reinforcing steel consists of hardened cement paste and of concrete aggregates (stone, sand). The cement paste and the aggregate are porous to a certain extent, and the pores are often partially filled with a water solution. This solution is rich in K,Na and Ca ions. If chloride ions arrive as a contaminant to the surface of the steel, the surface tends to become active when the molar ratio of Cl^- to hydroxyl ions in the pore solution reaches a critical value, thought to be about 0.3 [1,3,4]. Microscopically, the concrete acts as a non-homogeneous electrolyte. Macroscopically, the concrete may be viewed as a medium with an equivalent homogeneous resistivity which varies greatly (typically 10^3 to 10^7 ohm-cm) with the overall moisture content [5,6,7].

At the open circuit potentials normally encountered in steel and concrete, the reduction of oxygen is the most likely cathodic corrosion reaction [8]. To reach the surface of the steel, oxygen must be transported through the concrete cover. In the absence of cracks, this transport is expected to be by diffusion through the heterogeneous concrete matrix. The effective diffusion coefficient of oxygen through concrete has been reported to be dependent on the moisture content of the concrete, with values on the order of 10^{-5} cm^2/sec in concrete saturated with water. The effective diffusion coefficient is reported to be several orders of magnitude greater when the concrete has equilibrated with air at typical room humidities. Relatively few investigations have addressed these phenomena in relation to the extent of corrosion [8,9,10].

The anodic corrosion reaction is iron dissolution at the steel surface. Corrosion may be localized to a few mm^2, or extend over the length of the rebar, which could be many meters. In a structure containing mats of tied-together rebar, the steel can be an electrically continuous body extending over hundreds of square meters. The physical cross section, moisture content and chemical condition (for example, chloride content) of the concrete can vary significantly across the reinforced concrete assembly. This variation can generate complex corrosion macrocell patterns, which may shift with time, depending on weather changes and the service conditions.

Reinforcing Steel Bars

The concrete rebar commonly used is a pearlitic, hypoeutectoid material which is about 98% iron. Reinforcing steel bars may also be covered with an epoxy coating for corrosion protection. These epoxy-coated rebars (ECR) have been used extensively in the United States over the last one and a half decades. However, corrosion in these reinforcing bars may develop [11,12] if the coating has imperfections and the concrete is exposed to very aggressive environments. Galvanized rebars are also sometimes used in reinforced concrete construction [13,14]. Corrosion may also develop in this type of material under certain circumstances. Reinforcing bars with other types of coatings [15] or that are made out of other alloys, such as stainless steel [16,17], or non-metallic materials [18], are occasionally used. However, the vast majority of reinforcing steel bar applications have plain steel directly in contact with concrete.

Corrosion Evaluation

Because the rebar is embedded in a solid opaque medium, detection of corrosion and its

Corrosion pit sizes can equally be determined. In some instances, appearance ratings have been developed to provide a numeric descriptor of the overall rebar appearance.

Miscellaneous Methods

More recently, other corrosion-related spall or delamination detection techniques have been investigated. These and traditional techniques have been examined in detail as portions of the U.S. Strategic Highway Research Program [25]. Among recently implemented techniques is the use of radar for the detection of delamination of concrete within bridge decks. The use of laser-induced impact with acoustic monitoring on a non-contact basis has also been explored [25,26].

Determination of extent of corrosion of reinforcing steel in concrete can be done indirectly by measurement of the electrical resistance of embedded steel probes in the concrete. As the cross-section of the steel decreases because of corrosion, the electrical resistance of the embedded segment will also increase. This method, which encounters common use in other technologies such as the refinery industry [27], has been used sometimes to determine the overall corrosion condition [28] or the efficacy of cathodic protection systems [19]. Acoustic emission is another technique that has been examined as a possible method of establishing the corrosion rate of steel in concrete. As the corrosion-related expansion takes place, cracks in the concrete propagate in a discontinuous manner, creating acoustic signals that can be detected by an external detector [29]. This technique has not yet been widely used for this type of application.

Monitoring of the external dimensions of the concrete for detection of corrosion-induced stresses has been successfully achieved by means of strain gages placed in the external surface. The strain on the surface of the material can be related to the amount of corrosion product generated, thus providing an indication of the internal corrosion rate. This technique has been demonstrated for use in the laboratory for simple specimen geometries [30-32]. The technique can be highly sensitive, but it is affected by other related phenomena in the concrete, such as creep of the concrete and volume changes due to variations in the amount of moisture absorbed by the concrete.

ELECTROCHEMICAL TECHNIQUES

Static Measurements

The Potential Survey

When reinforcing steel is in the passive state, a mixed potential is achieved which is typically near -100 to -300 mV versus the copper/copper-sulfate (CSE) electrode. This mixed potential results from the interaction between the steel dissolution reaction, which proceeds at a slow rate in the passive regime, and the oxygen reduction reaction. As the reinforcing steel becomes active at localized regions (for example, where the chloride concentration has exceeded the threshold for activation), the dissolution of iron becomes faster there and the steel bar experiences an overall shift of its open circuit potential toward more negative values. This process is described in Figure 1. It would be expected that as a greater fraction of the steel surface becomes more active, the overall rebar potential will become more negative. Thus, the open circuit potential of reinforcing steel in concrete can be considered as a rough indication of the corrosion state of the system. This is the base of a commonly used criterion for the evaluation of the corrosion state of a reinforced concrete system, summarized by ASTM C876-91 "Standard Test Method for Half-Cell Potentials

of Uncoated Reinforcing Steel in Concrete" (the expression "half cell" is in common practice usage, not intended in the rigorous electrochemical sense). This procedure is based on numerous observations of open circuit potential in highway bridge decks, and correlation with those potentials with the actual extent of corrosion observed in the underlying steel.

In the laboratory there have been many observations of a relationship between corrosion rate and open circuit potential, lending credibility to the criterion under the appropriate circumstances [33,34]. However, the correlation is not universal, since a wide range of corrosion rate values are possible within a narrow range of open circuit potentials. In addition, once the surface of the reinforcing steel becomes fully active, the rate of metal dissolution is expected to actually decrease as more and more negative potentials are encountered, as in the kinetics of an anodic reaction under simple activation limitation. This situation takes place, for example, in reinforced concrete which is submerged in water, where the supply of oxygen through the concrete cover becomes limited by diffusion to a very small volume. In those cases, the surface of the steel may be fully active because of chloride ion contamination from the surrounding environment, while the steel is dissolving at a very low rate at highly negative potentials [35,36]. The possibility of other reduction reactions being present at a low potential regime has received some attention [50].

In field applications, it is actually possible to map the "half cell" potential over a large reinforced concrete surface. A connection is made to the reinforcing steel assembly and the difference of potential is made between the steel and a reference electrode that is placed consecutively at evenly spaced spots along the concrete surface. Because of the relatively high resistivity of the concrete, the "half-cell" potential will vary at different spots on the concrete surface, depending on the extent of steel corrosion underneath.

The actual distribution of potentials on the external concrete surface is not the same as the potential in the concrete which is immediately in contact with the steel surface. The spatial resolution of this technique depends on the resistivity of the concrete and the thickness of the concrete cover [37,38]. Figure 2 illustrates for a simple model case the computation of the expected potential distributions for electrodes that would be placed on the external surface of the concrete, compared with the distribution that would be expected if the electrodes were placed very close to the rebar surface [38]. As the Figure shows, the distribution of potentials becomes broader and therefore less defined at the external concrete surface. This convolution in the observed response of the system might explain why, at times, potential surveys have given misleading results for actual field systems.

Another possible cause of deviations of results is the presence of junction potentials. These potentials may be generated at the point of contact (sometimes made by means of an intermediate sponge). Deviations may also result from the presence of regions of different chemical makeup in the concrete, such as carbonated surface layers [39]. The extraneous potentials can at times reach magnitudes of several hundred millivolts.

Epoxy-coated rebar, galvanized rebar, and alternative rebar materials present unique electrochemical behavior situations for which a relationship between potential and corrosion state is not sufficiently established. Potential surveys for structures using those materials can therefore not be easily interpreted and unqualified use of standard procedures such as ASTM C-876 is not desirable.

In general, the potential survey method can be considered as a qualitative test of the

corrosion condition of plain steel bars in concrete. However, the results should not be taken uncritically as a definitive answer, or as an indication of the corrosion rate of the steel.

The Resistivity Survey

Because of the tendency for the formation of corrosion macrocells, the corrosion of steel in concrete is expected to become less severe as the concrete resistivity becomes greater, since the potential drop across resistive paths will be more pronounced. In addition, higher concrete resistivity is usually an indication of lower water content in the concrete. This means that less electrolyte will be available and thus the portion of the steel surface on which metal dissolution reactions could occur might be smaller [40,41].

Concrete resistivity surveys are conducted often in the field as a way of assessing the likelihood of corrosion developing in reinforced concrete structures. Criteria to interpret the results of the surveys vary, but it is generally recognized that the resistivity range from 20 K ohm-cm to 100 K ohm-cm represents a transition regime below which severe corrosion is possible and above which corrosion is only rarely observed [5,42]. Recently, quantitative correlations between concrete resistivity and corrosion rate have been examined with computational methods for extended macrocells [37,43], and the results correlated with measurements in laboratory columns partially submerged in salt water [12]. On first approximation, the total extent of corrosion in those systems appears to decrease with increasing concrete resistivity, but with a dependence weaker than a simple inverse proportion.

Concrete resistivity surveys can be viewed at present as an additional descriptor of the tendency of a system to develop rebar corrosion, but not as a sufficient means of assessing the extent or rate of the deterioration.

Measurement of Corrosion Macrocell Currents

The amount of electronic current flowing between anodic and cathodic regions of rebar corroding in concrete can at times provide an useful indication of the extent of corrosion activity. If separation between anodes and cathodes were complete (for example, metal dissolution taking place only at the upper rebar mat in a bridge deck, and oxygen reduction happening exclusively at the lower mat), then the current flowing between mats would give the total corrosion current by direct Faradaic conversion. Many laboratory test methods use this concept to monitor corrosion in applications such as rebar corrosion inhibitor evaluation, testing of new rebar corrosion control coatings, and long term corrosion monitoring [15,94,95]. These measurements can also be used in the field if connections between different parts of the rebar assembly can be safely broken for current measurement. The currents are usually measured by means of a low resistance shunt or zero-resistance ammeter.

This method has the advantage of providing direct indication of electrochemical activity in the system, without the need for highly sophisticated instrumentation. The main drawback is that the individual rebar regions, while certainly operating as net cathodes or anodes, may be acting as mixed potential electrodes because of combined cathodic and anodic activities. In a worst case situation, both rebar regions might be corroding at a high rate, with only a small imbalance current flowing between the two of them. It has been estimated that corrosion current underestimation may be as much as by one order of magnitude [96]; recent calculations of extended systems with long range macrocells predict similar effects [43,86].

Caution should be used in interpreting the results of this type of measurement, especially when attempting to predict the long-term behavior to new corrosion control methods. The simultaneous use of other measurement techniques is advisable.

Electrochemical Noise

The electrode potential of a corroding system fluctuates with time, especially if processes such as pit origination and repassivation take place. The potential of corroding rebar in concrete can fluctuate slightly (typically in the sub-mV range) within time intervals on the order of seconds, and by as much as several hundred mV over days or weeks [67]. Analysis of the fluctuations both in the time domain and after spectral decomposition can provide indirect indication of the average rate of corrosion of the system. Application of this technology to steel in concrete is in a relatively early stage, and reliable, long term quantitative correlations between noise signatures and corrosion rate have yet to be developed [90].

Polarization Measurements - Large Amplitude.

Polarizations Scans

Because of the electrochemical nature of rebar corrosion, it is possible to obtain corrosion rate information by means of the application of external electrical stimuli and determination of the electrical response of the system. A number of well established test techniques could be applied if certain simplifying conditions were met. For example if :

1. The system behaves as a discrete mixed potential electrode (that is, no spacial separation or finite electrolyte resistance exists between anodic and cathodic sites)

2. Both the cathodic and the anodic reactions are subject to simple activation polarization

3. The corrosion potential is far enough removed from the respective equilibrium potentials of the species being reduced and oxidized in the corrosion reaction, so that the reverse reactions can be neglected

4. Any deviations from steady state corrosion are made slowly enough that currents to charge/discharge interfacial capacitances can be ignored

then the current density i_{ap} that needs to be applied to the steel to deviate from its corrosion potential E_{corr} by an amount E_{dev} is given by

$$i_{ap} = i_{corr} [\exp (2.3 E_{dev}/b_a) - \exp (-2.3 E_{dev}/b_c)] \qquad (1)$$

where b_a and b_c are the anodic and cathodic Tafel slopes respectively. If the absolute value of E_{dev} is large enough, then there is a linear relationship between E_{dev} and $\log(i_{ap})$, with a graphic slope equal to b_a or b_c depending on the sign of E_{dev}. Linear extrapolation to $E_{dev}=0$ yields therefore i_{corr}. This is the basis for the Tafel extrapolation method of corrosion rate determination, whereby i_{ap} is applied by means of an external power source and the values of the resulting E_{dev} are measured

and recorded for analysis and extrapolation.

Tafel slope extrapolation has been used with success to determine corrosion rates of metals in contact with free liquid electrolytes, but not often in concrete [44]. Severe difficulties develop because the system does not usually meet the simplification requirements. If the potential excursion is in the anodic direction, there is danger of irreversibly triggering pitting during the test if an otherwise subcritical chloride concentration is present at the steel surface. If the excursion is conducted instead in the cathodic direction, capacitive effects may still require impractical low potential scan rates to avoid excessive error. Because of slow oxygen diffusion in concrete, the cathodic reaction may also be affected by significant concentration polarization. This could introduce sizable complication in two ways. First, the polarization behavior could become highly time-dependent and cause additional need for very slow measurements. Second, the relationship between E_{dev} and E_{app} becomes more complicated than that given by Eq. (1) and practical application of the method may not be feasible (if the system is under complete diffusional control a simplification making b_c = infinity can be attempted).

Additional difficulties are created by the finite resistivity of concrete and the presence of corrosion macrocells. The concrete resistivity creates ohmic potential differences between points at the steel surface and the point at which the reference electrode is placed to perform the E_{dev} measurements. Unfortunately, because the system is spatially distributed and also contains corrosion macrocells, it is not possible in most cases to simply eliminate the ohmic polarization component by current interruption or comparable techniques. Current distribution effects in the presence of macrocells on steel in concrete can lead to gross distortion in the shape of E-log i diagrams when performing measurements with and without current interruption [45].

Other complications can result from variations in the relative size of anodic to cathodic areas during polarization [46], and the onset of other electrochemical phenomena as the potential changes significantly from the initial E_{corr} range.

In some instances it is possible to account for part of the time-dependant effects by means of cyclic potentiodynamic E-log i tests followed by computation and separation of the non-Faradaic currents. This has been done with success for steel segments where only the cathodic reaction is present and is uniformly distributed [47]. Rapid scan, large signal polarization methods have been useful for applications such as evaluation of rebar corrosion inhibitors [48,49]. Nevertheless, because of the complications mentioned above, Tafel extrapolation and large signal methods in general are not widely used at present in reinforced concrete for corrosion rate determination.

Polarization Measurements - Small Amplitude.

Basic Aspects and the Polarization Resistance Method

Small amplitude polarization measurements (with potential deviations from local static potential much smaller than the magnitude of the activation Tafel constants) in concrete tend to avoid permanent system upsets and permit, at times, better control of the errors that are due to high electrolyte resistivity. These methods take advantage of the quasi-linear relationship between applied current and potential deviation that may be encountered when the latter is small. For example, if the assumptions leading to Eq. (1) are satisfied, E_{dev} is very small, and the reference electrode is placed immediately next to the metal surface, then the equation reduces to [51]:

$$E_{dev}/i_{ap} = B/i_{corr} \quad (2)$$

with

$$B = b_a b_c/2.3\ (b_a+b_c) \quad (3)$$

in this particular case.

This is a form of the Stern-Geary equation, showing that the ratio of the potential deviation to the applied current density is inversely proportional to the corrosion current density. The ratio E_{dev}/i_{ap} obtained in this case is equal to the polarization resistance (Rp) of the system, which is defined as the limit value of the ratio when the potential is varied at an infinitely slow rate, at the small amplitude limit. The magnitude B in Eq. (3) is a simple function of the Tafel slopes. Comparable relationships exist for other cases. For example, if the previous assumptions hold but the cathodic reaction is completely under diffusional control, then $B=b_a/2.3$ [52].

Approximate values of the activation parameters are often known beforehand, thus providing values of B if an appropriate expression linking B with those parameters is known to be valid. Therefore in cases where Eq. (2) is valid and the value of B can be obtained, corrosion rates can be determined by means of relatively quick and non-destructive measurements. This is the basis for the Polarization Resistance (PR) method of corrosion rate measurement. Its limitations will be discussed in the light of the overall response of a system to external signals, detailed below.

The Electrochemical Impedance Response

To understand some of the limitations of the PR method, and to obtain clues as to how to compensate for some of the sources of error, it is desirable to examine the behavior of the system from the more general standpoint of the dynamic response to small signal excitations. Information on that behavior can be obtained from electrochemical impedance spectroscopy (EIS) measurements, which can also be used directly for the evaluation of corrosion rates.

In the EIS measurement a small-signal, harmonic variation of the potential of the system is created by means of an externally imposed alternating current. Measurements of the amplitude and phase angle of both the excitation current and the potential variation are made at various frequencies, covering an spectral range extending typically from 1 mHz to 1 kHz or more. At each test frequency, the electrochemical impedance **Z** is defined as the complex vector equal to the ratio of the potential response phasor (**V**) to the excitation current density phasor (**i**) [53,54].

Availability of EIS information over a wide frequency range can be helpful in separating the effect of complicating factors, from those elements in the system response that can be used to evaluate corrosion rate. For example, at the high frequency limit behavior the interfacial capacitances across the corroding interface offer a very low impedance path so that the Faradaic processes responsible for corrosion do not contribute to the system response. The overall impedance is then determined, at the high frequency limit, by the effective ohmic resistance of the electrolyte between the point where the reference electrode is located and the surface of the metal. This limit can then be conveniently subtracted from the rest of the spectrum. If the system is not spatially distributed, the remaining spectrum is not affected by the electrolyte resistance, facilitating interpretation of results.

Figure 3 shows the predicted EIS response of a discrete system satisfying conditions (1) and (3) in the Large Amplitude section, but where condition (2) is satisfied only by the anodic reaction [55-57]. The cathodic reaction is allowed to experience mixed activation-concentration control. The system is assumed to possess also a finite interfacial capacitance and a finite electrolyte resistance Rs between the reference electrode and the metal. In spite of these complications, the limiting behavior of various frequency regimes provides information with which to evaluate the corrosion current density. Under complete diffusional control the evaluation of i_{corr} could be performed independently from two different limit values.

Complications in PR Method Measurements - Discrete Systems

A PR measurement would in principle involve a simple deviation of the system from its corrosion potential, observation of the required current, and calculation of R_p leading to i_{corr} by Eq. (2). Unfortunately, many of the complicating factors indicated in the Large Amplitude excitation section are still present and evaluation of corrosion rates by PR can be involve significant error. Causes of error are discussed below that can act in discrete systems, where separation between anodic and cathodic areas and other current distribution effects can be neglected. The additional difficulties that may result from extended system geometries will be treated subsequently.

Figure 3 serves to illustrate some complicating factors. If the potential scan rate in a PR measurement is low enough, R_p will have a value approaching the low-frequency limit of the impedance (minus Rs). However, unlike EIS, the PR technique provides no indication of the extent of diffusional polarization that might be present. Therefore, Rp could be related to the corrosion rate through a B constant that can range between the two extremes corresponding to complete diffusional control and complete activation control. Assuming typical likely values for ba and bc of 60 mV and 160 mV [52], the possible values of B would range between 20 mV and 26 mV for the two extreme cases. Choosing an intermediate value would result in an error, although of relatively small magnitude.

More important errors may result depending on how well PR measurements approach the equivalent of the low-frequency impedance limit. It is often of interest to detect corrosion early, when typical corrosion current densities may be on the order of 0.1 $\mu A/cm^2$ [20,21]. In a typical PR test with a scan range of 10 mV, this would result in maximum Faradaic currents of about 0.5 $\mu A/cm^2$. Representative potential scan rates in PR measurements are on the order of 0.1 mV/sec, while effective interfacial capacitances on rebar tend to be on the order of 1,000 $\mu F/cm^2$ [52]. As a result, during the test non-Faradaic currents of ~1 $\mu A/cm^2$ could develop, overshadowing the Faradaic component, and consequently leading to erroneous estimates of Rp.

Errors due to interfacial capacitance effects (if the capacitance approaches ideal behavior) can be reduced by careful control of the potential scan procedure with appropriate solution resistance compensation schemes. The contribution of the non-Faradaic component of the current would then be reduced to simply an offset in the polarization plot, or accounted for by means of extrapolation procedures as a function of excitation rate. Several test approaches have been developed for this purpose, including the use of cyclic polarization techniques [20,33,58-60]. Pulse excitation techniques, potentiostatic, galvanostatic, or using coulostatic control have also been used to obtain better approximations to the value of Rp [49,61,62].

The PR methods and related pulse techniques adjusted for interfacial capacitance and solution resistance often assume that the system behaves as having a single time constant, thus

permitting estimation of Rp by means of relatively short measurements. That is equivalent to extrapolating from the behavior in the high frequency end of the semicircle in Figure 3, to obtain the value of the low frequency limit. The procedure is therefore subject to error from the existence of low frequency features, such as that generated by the diffusional component of the spectrum. Further complication results because interfacial capacitance of rebar can be markedly non-ideal, as illustrated in Figure 4 [63]. The apparent capacitance values may greatly exceed those expected from simple surface roughness predictions, suggesting the presence of complex interfacial behavior [64-67]. As a result, the impedance behavior presents normally significant frequency dispersion, even in the absence of macroscopic current distribution effects. Extrapolation from short PR or pulse experiments to obtain Rp is consequently less certain, and could give rise to sizable errors in the estimation of corrosion rate. Errors in estimating Rp will tend to become larger also as the concrete resistance increases relative to the value of the Faradaic impedance of the system, since the estimated value of Rp will result from the difference between magnitudes comparatively close to each other.

Excitation Current Distribution Effects.

The discussion above was limited to a discrete system displaying some of the characteristics of reinforcing steel in concrete. Unfortunately, actual structures do not behave as a discrete mixed potential electrode. The combination of relatively high electrolyte resistivity with macroscopic component sizes causes complicated current distribution patterns to develop. The response of the system to an electrochemical excitation is then the sum of numerous responses from individual surface elements, each with a different polarization condition and excited differently by the test signal.

Evidence of this complication is observed in the EIS test results shown in Figure 5 [63-69]. The Nyquist diagram in figure 5A resembles a single semicircle, as it would be expected from the medium-to-high frequency behavior predicted in Figure 3. However, there is considerable distortion at the high frequency end, where the diagram meets the real axis at an angle approaching 45°. Results from testing a different specimen are shown in Figure 5B. There the high frequency distortion is also present, but in addition the diagram shows no indication of converging toward a real value at the low frequency limit.

The high frequency distortion may be explained as being the result of the combination of high concrete resistivity, macroscopic specimen sizes, and the presence of appreciable interfacial capacitance (which may have some frequency dispersion of its own, as shown earlier). The impedance response of a long concrete beam containing a longitudinal rebar will be considered as an illustration. As shown schematically in Figure 6, the portions of the bar closer to the excitation point receive a large fraction of the excitation current than those bar portions further away. A simplified model of that situation is presented in Figure 7, where the beam has been divided into longitudinal elements of length dx. Each element has an admittance $dY = Y_l\, dx$, where Y_l is the admittance per unit length. The corresponding element impedance is $dZ = 1/dY$; the magnitude Z_l can be defined so that $dZ = Z_l/dx$. Each element has also a longitudinal resistance $dR = R_l dx$, where R_l is the resistance per unit length which is a function of the concrete resistivity and the beam cross-section. This equivalent circuit has the characteristics of an electric transmission line, and has been used to model a variety of electrochemical systems [70-72]. If the beam has a length L, and if both Z_l and R_l are constant along the beam, the overall impedance Z_t measured from one of the ends is given by the de Levie relationship [72,73]:

$$Z_t = (R_l Z_l)^{1/2} / \tanh (L (R_l/Z_l)^{1/2}) \qquad (4)$$

which, if L is large becomes simply:

$$Z_t = (R_l Z_l)^{1/2} \qquad (5)$$

Figure 8 shows schematically the impedance diagrams expected from Eqs. (4,5) for systems with no corrosion (Z_l corresponding only to interfacial capacitance) and undergoing corrosion (Z_l assumed to correspond to a parallel combination of interfacial capacitance and polarization resistance [72]). The distributed impedance of the interfacial capacitance causes the phase angle of the measured impedance to be close to 45° at the high frequencies. This is a likely cause of the high-frequency semicircle distortion exemplified in Figure 5A and 5B. The low-frequency limit behavior of Z_t is related to the low-frequency limit of Z_l by Eqs.(4,5). Figure 8 shows the low frequency limit value of Z_t for a simple case where Z_l is the parallel combination of a distributed polarization resistance R_{pl} and a distributed interfacial capacitance C_l. The data in Figure 5A might be viewed as corresponding to that case. Experimental determination of the low-frequency limit of Z_t, together with knowledge of R_l would thus permit obtaining R_{pl}, and from there determining the corrosion current per unit bar length by application of Eq. (2).

Methods based on the above approximation were presented by Feliu et al [74-76] to calculate the uniform distributed polarization resistance for reinforced concrete beams and slabs. One- and two-dimensional transmission line configurations were assumed for the beam and slab cases respectively. Potentiostatic step excitation, as in PR measurements, was considered by those investigators to provide enough approximation to the low-frequency limit to ignore reactive impedance effects.

There are instances, however, when the impedance of corroding rebar in concrete displays significant reactive impedance even at very low frequencies, without clearly converging toward a real limit (as in Figure 5B). Sometimes the impedance of corroding rebar at low frequencies approaches the behavior of a constant phase element (CPE) with a phase angle near 45° [33,77,78], even when the specimen configuration cannot be represented well by a semiinfinite transmission line. This type of behavior resembles the low-frequency diffusional impedance observed in some equilibrium electrodes [79,80] or predicted for mixed-potential systems with both reactions subject to diffusional limitation [55]. That has led to modeling the Faradaic component of the impedance by means of a series combination of a diffusional Warburg term and a charge-transfer resistance [77,81]. Difficulties with this concept exist because the rebar surface is expected to be significantly removed from equilibrium, and the iron oxidation reaction is not thought to be under diffusional control [56,57,82]. Under such conditions, the diffusional term would not be dominant. In principle, a parallel combination model such as the one shown in Figure 3 would be more adequate but it fails to predict a dominant diffusional impedance behavior at the low frequencies.

Recent modeling of the impedance of rebar in concrete has provided insight in resolving the apparent inconsistencies discussed above. Macdonald and coworkers [83-85] have presented calculations that combine both a diffusional component of the impedance with a transmission-line configuration. In that concept, the rebar surface is divided into individual elements each with its own characteristic impedance which includes a diffusional term. The elements are linked by resistive concrete components forming a transmission line. The model predictions reproduce experimental observations such as those in Figure 5B. Deconvolution procedures to identify the

distributed corrosion current are also presented.

An integrated approach by Kranc and Sagüés [38,86] has extended modeling to multidimensional systems by first computing the static corrosion and oxygen reduction current distribution over the rebar, and then evaluating the combined impedance of the macroscopic system. The individual impedance elements conform to elements of the model in Figure 3, developed starting from a simplified version of the concentration-overpotential equation. The results show that if the anodic area on the rebar surface is small compared with the cathodic area, the high resistivity of concrete may cause preferential excitation of the cathodic regions when compared with the case of a discrete mixed-potential electrode. This is roughly equivalent to having a greater ohmic resistance in series with the anodic portion of the impedance, and consequently emphasizing the diffusional (cathodic) impedance response of the system. As shown in Figure 9, the result is an increased phase angle at low frequencies compared with the discrete system case. Another important consequence is that the interfacial capacitance of the rebar surface causes the cathode-anode current distribution ratio to change with frequency (See Figure 10). At the high-frequency limit the measured ohmic resistance is less than at lower frequencies [87]. Because the charge-transfer resistance is evaluated by the difference between high and low frequency impedance values, this can result in significant underestimation (for example by a factor of 3) of corrosion current densities if rebar corrosion is localized.

The current distribution effects mentioned above can create additional complications (both in large and small size systems) which must be kept in mind when using PR or short-time pulse measurement techniques. Because these techniques are equivalent to examining only very small portions of the impedance spectrum, indications of severe complicating factors might be missed and erroneous interpretation of data can result. Preliminary EIS measurements, if feasible, would be highly desirable if simpler techniques are contemplated for later routine use in a particular application.

Current confinement ("guard") electrodes.

Corrosion measurement uncertainties due to current distribution effects could be minimized if the excitation current were to be limited to a region of known dimensions in an otherwise extended reinforced concrete structure. Additional electrodes, typically in the form of a guard ring around the counter electrode, have been used for that purpose. The guard electrode is polarized at the same potential as the counter electrode, but connected to an independent signal source. If the guard electrode is large enough and if the impedance at the metal surface and electrolyte resistance are uniformly distributed, then the counter electrode current will flow only to the portion of the metal surface directly underneath the counter electrode [88-90]. If those conditions are met, the measurement will correspond only to a well-defined area, and accurate charge transfer rate measurements could be achieved. Unfortunately, uniform corroding conditions are rarely the case in extended concrete systems, and the excitation current of the area below the counter electrode may differ markedly from that supplied by the counter electrode. Of special interest is the case of a relatively small corroding spot surrounded by a large passive steel region. Calculations for this configuration have been reported by Kranc and Sagüés [91]. The results show that at high test frequencies, when the impedance of the interface is primarily capacitive and relatively uniform, current distribution is properly controlled by the guard electrode. At low test frequencies the corroding spot, because of its lower specific impedance, receives current not only from the counter electrode but also from the surrounding ring. This causes significant underestimation of the corrosion current density of the active spot in the cases examined. Similar calculations for an

uniformly corroding system showed, as expected, that current confinement is adequate.

Evaluation of the effectiveness of guard ring electrodes to improve corrosion rate measurement accuracy under practical conditions have been conducted in field tests under the SHRP program [25,84]. The results indicated that devices using guard ring electrodes gave corrosion rates about one order of magnitude lower than those obtained with unconfined electrodes. Correlation with field corrosion rates evaluated by direct observation is desirable but not yet sufficiently confirmed.

ADDITIONAL ISSUES

The items reviewed in the previous sections are major issues in the way of reliable measurements of corrosion in concrete. Important concerns not addressed in this paper include the role of corrosion products on the electrochemical response of the system to external excitation, the effect of potential drops at concrete layers near the steel surface or at the outer concrete surface, the electrical inhomogeneity of the paste-aggregate environment, and the complications involved in measuring corrosion of polymer-coated reinforcing steel [92,93]. Numerous problems remain to be solved in the practical application of electrochemical techniques to structures in the field, including reliable electrodes and contacts, electromagnetic interference and stray currents, choice of stable reference electrodes and the development of adequate monitoring equipment. In addition to the measurement problem itself, the choice of a measurement schedule that will provide a representative sampling of short and long term environmental conditions is another challenge that remains to be addressed.

SUMMARY

1) Non-electrochemical test techniques tend to detect corrosion of steel in concrete when the deterioration is at relatively advanced stage. As a result, these techniques are most useful for the purpose of assessing the extent of needed rehabilitation or as a warning of possible damage in similar structures. Some potentially more sensitive non-electrochemical techniques such as acoustic emission and external strain monitoring are in need of additional development.

2) Observational electrochemical techniques can be very sensitive and, in the case of macrocell current measurements, provide direct evidence of corrosion activity. Potential surveys are widely used for field corrosion assessment and can provide very useful, early indication of corrosion initiation. However, complications in the system behavior are present and potential surveys should not be taken uncritically as a definitive determination of the corrosion state of the steel. Concrete resistivity surveys can provide general indications of the likelihood of corrosion development.

3) The suitability of measurements of corrosion rates of corroding steel in concrete, by means of excitation-response electrochemical measurements was discussed. Simple linear polarization or potential step measurements would be adequate to evaluate corrosion rates when the corroding system behaves as a simple, discrete mixed potential electrode. However, current distribution effects coupled with the presence of a large reactive component of the interfacial impedance can result in a highly convoluted polarization response of steel in concrete under many conditions. This situation often tends to preclude the use of simple polarization measurements to evaluate corrosion rates of steel in concrete, unless some prior information on the impedance response of the system already exists to reveal the extent of complicating factors.

4) Corrosion rate evaluation by means of sophisticated methods of impedance measurement and analysis appears to be feasible. The implementation of this approach is only now beginning to be attempted, and considerable experimental verification will be needed to establish the value of this approach. Knowledge of the actual polarization conditions present on steel in concrete (such as for example the extent of diffusional polarization, or the value of the interfacial capacitance) is necessary for the successful application of any measurement technique. This kind of information is not sufficiently available at present.

5) Methods based on excitation current confinement show promise in simplifying the system response so that only a restricted portion of steel is being examined. thus facilitating corrosion rate evaluation. At this time there is not enough information available to safely predict the extent of current confinement in each practical condition (for example, if more than one mat of reinforcing steel is present below the counter electrode). Additional development and verification will be necessary in this area.

BIBLIOGRAPHY

1. Schiessl, P., Editor, "Corrosion of Steel in Concrete", Report of the Technical Committee 60-CSC RILEM, Chapman and Hall, London, 1988.

2. Mehta, P. K., "Concrete: Structure, Properties and Materials", Prentice-Hall, Englewood Cliffs, N.J., 1986.

3. Slater, J., "Corrosion of Metals in Association with Concrete", ASTM STP 818, ASTM, Philadelphia, 1983.

4. "Corrosion of Metals in Concrete", ACI Journal Committee Report by ACI Comm. 222, Journal of the American Concrete Institute, p.3, Proceedings Vol.82, 1985.

5. Browne, R., "Mechanisms of Corrosion of Steel in Concrete in Relation to Design, Inspection and Repair of Offshore and Coastal structures", in Performance of Concrete in Marine Environment, Publication SP-65, American Concrete Institute, Detroit, 1980.

6. Stratfull, R., Materials Protection, p. 29, March 1968.

7. Millard, S. G., Ghassemi, M., Bungey, J. and Jafar, M., "Assessing the Electrical Resistivity of Concrete Structures for Corrosion Durability Studies", in Corrosion of Reinforcement in Concrete, C. Page, K. Treadaway and P. Bamforth, Eds., p.303, Elsevier Appl. Sci., London-New York, 1990.

8. Tuutti, K., Corrosion of Steel in Concrete, Swedish Cement and Concrete Research Institute, 1982.

9. O. Gjorv, O. Vennesland and A. El-Busaidy, Materials Performance, Vol.25, No.12, p.39 (1986).

10. Morehead, W., Diffusion of Dissolved Oxygen through Concrete (Discussion), Materials Performance, Vol.26, No.5, p.34, 1987.

11. Sagüés, A., Powers, R., Zayed, A., "Marine Environment Corrosion of Epoxy-Coated Reinforcing Steel", in Corrosion of Reinforcement in Concrete, C. Page, K.Treadaway and P. Bamforth, Eds., pp.539-549, Elsevier Appl. Sci., London-New York, 1990.

12. Sagüés, A. , Perez-Duran. H. and Powers, R., Corrosion, Vol 47, p.884, 1991.

13. Cornet, I. and Bresler, B., "Galvanized Steel in Concrete: Literature Review and Assessment of Performance", International Lead Zinc Research Organization, New York (1981).

14. A. Macias and C. Andrade, Corrosion Sci., Vol 30, p.393, 1990.

15. "Corrosion Performance in Concrete of Reinforcing Steel with a Protective Inorganic Coating", A. Sagüés, B. Boucher and X. Chang, Paper No. 197, Corrosion/92, National Association of Corrosion Engs., Houston, 1992.

16. Rasheeduzzafar, Dakhil, F., Bader, M. and Khan, M., ACI Materials Journal, Vol. 89, p. 439, 1992.

17. Treadaway, K., Cox, R., and Brown, B., "Durability of Corrosion Resisting Steels in Concrete", Proc. Instn. Civ. Engrs., Part I, p.305, Vol 86, April 1989

18. Chaallal, O. and Benmokrane, B. "Glass-Fiber Reinforcing Rod: Characterization and Application to Concrete Structures and Grouted Anchors", p.606 in Materials: Performance and Prevention of Deficiencies and Failures, Proc. of the Materials Eng. Congress, Atlanta, Aug. 10-12, 1992, American Society of Civil Engineers, New York, 1992.

19. Stratfull, R., "Criteria for the Cathodic Protection of Bridge Decks", in "Corrosion of Reinforcement in Concrete Construction", p. 287, A. P. Crane, Ed., Ellis-Horwood, Chichester, 1983.

20. Clear, K. Measuring Rate of Corrosion of Steel in Field Concrete Structures, TRB 68th Annual Meeting, January 22-26, 1989, Paper Preprint No. 88-0324.

21. Andrade, C., Cruz Alonso, M. and Gonzalez, J., "An Initial Effort to Use the Corrosion Rate Measurements for Estimating rebar Durability", p.29 in Corrosion Rates of Steel in Concrete, ASTM STP 1065, N. Berke, V. Chaker and D. Whiting, Eds., ASTM, Philadelphia, 1990.

22. R. Weyers, P.I., SHRP Contract C-103, "Concrete Bridge Protection and Rehabilitation: Chemical and Physical Techniques", Final Report, to be published 1993, Strategic Highway Research Program, National Research Council, Washington, 1993.

23. Sagüés, A., "Critical Issues in Electrochemical Corrosion Measurement Techniques for Steel in Concrete", Paper No.141, Corrosion/91, National Association of Corrosion Engineers, 1991.

24. Sack, D., Olson, D. and Phelps, G., "Innovations for NDT of Concrete Structures", p. 519, in Materials: Performance and Prevention of Deficiencies and Failures, Proc. of the Materials Eng. Congress, Atlanta, Aug. 10-12, 1992, American Society of Civil Engineers, New York, 1992.

25. Cady, P., "Condition Evaluation of Concrete Bridges Relative to Reinforcement Corrosion", Final Report Contract C-101, Vols. 1-8, SHRP-S/FR-92-103 to 110, Strategic Highway Research Program, National Research Council, Washington, 1992.

26. Little, V., "Evaluation of the Use of Laser Ultrasonics for the Rapid, Noncontact Inspection of Concrete and Asphalt", Final Report, SHRP-ID/UFR-92-604, Strategic Highway Research Program, National Research Council, Washington, 1990.

27. Barnett, W.P., Sagüés, A.A., Davis, B.H., and Baumert, K., Fuel Processing Technology, 8, pp. 53-64, 1983.

28. Rincon, O. , Sanchez, M., Montiel, E. and Nunez, M. "Evaluation of Problems Associated with a Cast Wall Pier", (*in Spanish*), Paper T-9, Proc. of 1st. Symposium on Reinforced Concrete Structures, Maracaibo, Venezuela, 7-9 October, 1992, Centro de Estudios de Corrosion, University of Zulia, Maracaibo, Venezuela.

29. Hartt, W., Dunn, S., Weng, M. and Brown, R., "Application of Acoustic Emission to Detection of Reinforcing Steel Corrosion in Concrete", Paper No. 49, Corrosion/81, National Assoc.of Corrosion Engs., Houston, 1981.

30. Pickering, H., Corrosion, Vol.42, p.125, 1986.

31. Pangrazzi, R., Ducrocq, L., Hartt, W., and Kessler, R., "An Analysis of Strain Changes in Cathodically Polarized Pretensioned Concrete Specimens", Paper No. 554, Corrosion/91, NACE, Houston, 1991.

32. Lee, J.B. and Sagüés. A., to be published.

33. Aguilar, A., Sagüés, A. and Powers, R. Corrosion Measurements of Reinforcing Steel in Partially Submerged Concrete Slabs, in Corrosion Rates of Steel in Concrete, N.Berke, Ed., STP 1065, ASTM, Philadelphia, 1990.

34. Escalante, E., "Effectiveness of Potential Measurements for Estimating Corrosion of Steel in Concrete", p.281, in Corrosion of Reinforcement in Concrete, C. Page, K.Treadaway and P. Bamforth, Eds., Elsevier Appl. Sci., London-New York, 1990.

35. Browne, R., Geoghegan, M., and Baker, A., "Analysis of Structural Condition from Durability Results", p.193, in Performance of Concrete in Marine Environment, Publication SP-65, American Concrete Institute, Detroit, 1980.

36. Preece, C., Gronvold, F. and Frolund, T., "The influence of Cement Type on the Electrochemical Behaviour of Steel in Concrete", in "Corrosion of Reinforcement in Concrete Construction", p. 393, A. P. Crane, Ed., Ellis-Horwood, Chichester, 1983.

37. Naish, C., Harker, A. and Carney, R., "Concrete Inspection: Interpretation of Potential and Resistivity Measurements", in Corrosion of Reinforcement in Concrete, C. Page, K. Treadaway and P. Bamforth, Eds., p.314, Elsevier Appl. Sci., London-New York, 1990.

38. Kranc, S.C. and Sagüés, A.A., "Computation of Corrosion Macrocell Current Distribution and Electrochemical Impedance of Reinforcing Steel in Concrete", in Computer Modeling in Corrosion, ASTM STP 1154, R.S. Munn, Ed., American Society for Testing and Materials, Philadelphia, p.95, 1992.

39. Bennet, J., and Mitchell, T., "Reference Electrodes for use with Reinforced Concrete Structures" , Paper No.191, Corrosion/92, National Assoc. of Corrosion Engineers, Houston, 1992.

40. Alonso, C., Andrade, C. and Gonzalez, J., Cement and Concrete Research, Vol. 8, p. 687, 1988.

41. Andrade, C., and Alonso, C., "Values of Corrosion Rate of Steel in Concrete in Order to Predict Service Life of Concrete Structures", in "Application of Accelerated Corrosion Tests to Service Life Prediction of Materials", STP 1194, G. Cragnolino, Ed., ASTM, Philadelphia, 1992.

42. Millard, S.G., Durability Performance of Slender Reinforced Coastal Defense Units, in Concrete in Marine Environment, p.339, V. Malhotra, Ed., ACI SP-109, American Concrete Institute, Detroit, 1988.

43. Kranc, S. and Sagüés, A., "Computation of Reinforcing Steel Corrosion Distribution in Concrete Marine Bridge Substructures", Paper No. 327, Corrosion/93, National Assoc. of Corrosion Engs., Houston, 1993.

44. Schell, H. and Manning, D., Materials Performance, Vol. 24, p.18, July 1985.

45. Sagüés, A. and Kranc, S.C., Corrosion, Vol. 48, 1992.

46. Root, C.R., "The Role of Oxygen in the Corrosion of Steel in Concrete", M.S. Thesis, University of Oklahoma, Norman, Oklahoma, 1981.

47. Al-Mansur, A.K.M. "Effect of Moisture Application on the Corrosion Behavior of Reinforcing Steel in Marine Bridge Substructures", M.S. Thesis, University of South Florida, Tampa, Florida, December, 1992.

48. Locke, C. and Rincon, O. "A Study of Corrosion Electrochemistry of Steel in Chloride Contaminated Concrete Using a Rapid Scan Polarization Technique", Paper No. 128, Corrosion/87, National Assoc. of Corrosion Engs., Houston, 1987.

49. Sanchez, M. and Rincon, O., "Techniques Used for Corrosion Monitoring in Steel-Reinforced Concrete Strctures" (*in Spanish*), Paper T-1, Proc. of 1st. Symposium on Reinforced Concrete Structures, Maracaibo, Venezuela, 7-9 October, 1992, Centro de Estudios de Corrosion, University of Zulia, Maracaibo, Venezuela.

50. Gonzalez, J.A., Molina, A., Otero, E. and Lopez, W., Magazine of Concrete Research, Vol. 42, No. 150, p.23, 1990.

51. Uhlig, H., and Revie, R., Corrosion and Corrosion Control, 3rd. Ed., John Wiley, New York, 1985.

52. Mansfeld, F.,"The Polarization Resistance Technique", in Advances in Corrosion Science and Technology, Vol. 6, M. Fontana and R. Staehle, Eds., Plenum Press, New York, 1976.

53. D.Macdonald and M. McKubre "Electrochemical Impedance Techniques in Corrosion Science",in Electrochemical Corrosion Testing, p.110, ASTM STP 727, F. Mansfeld and U. Bertocci, Eds,. ASTM, Philadelphia (1981).

54 Epelboin, I., Gabrielli, C., Keddam, M. and Takenouti, H., "AC Impedance Applied to Corrosion Studies", in Electrochemical Corrosion Testing, p.150, ASTM STP 727, F. Mansfeld and U.Bertocci, Eds,. ASTM, Philadelphia (1981).

55. S. Haruyama, "Faradic Impedance of Mixed Potential Electrode," Proc. Fifth Int. Cong. Metallic Corrosion, p.82, National Association of Corrosion Engineers, Houston (1974).

56. T. Tsuru, "Treatment of Diffusion Impedance in AC Impedance Method", 61st. Japan Soc. Corr. Eng. Symposium Report, pp.97-106 (1985).

57. A. A. Sagüés, Corrosion Vol 44, 555 (1988).

58. Macdonald, D., J. Electrochem. Soc., Vol.,125, p.1443, 1978.

59. Shih, H., and Pickering, H., J. Electrochem. Soc., Vol 134, p.1943, 1987.

60. Shih, H., and Pickering, H., J. Electrochem. Soc., Vol. 134, p.1949, 1987.

61. Gonzalez, J., Molina, A., Escudero, M. and Andrade, C., Corrosion Science, Vol 25, p. 519, 1985.

62. Gonzalez, J., Molina, A., Escudero, M. and Andrade, C., Corrosion Science, Vol 25, p. 917, 1985.

63. Sagüés, A., Electrochemical Impedance of Corrosion Macrocells on Reinforcing Steel in Concrete, Paper No. 132, Corrosion/90, Nat. Assoc. of Corr. Engs., Houston, 1990.

64. Shreir, L., Editor, Corrosion, Volume 1, Metal/Environment Reactions, Newnes-Butterworths, London, 1976.

65. Rammelt, U., and Reinhard, G., Corrosion Science, Vol.27, P.373, 1987.

66 Matthew Thomas, "Effect of Surface Roughness on the Double Layer Capacitance at The Steel/Alkaline Medium Interface", M.S. Thesis, University of South Florida (1988)

67. J. Dawson, "Corrosion Monitoring of Steel in Concrete", in Corrosion of Reinforcement in Concrete Construction, A.Crane, Ed., Ellis

Horwood, Chichester (1983).

68. Andrade, C. and Gonzalez, J., Werkstoffe un Korrosion, Vol. 29, p.515, 1978.

69. Sagüés, A. to be published.

70. D. Macdonald, M. McKubre and M. Urquidi-Macdonald, Corrosion, Vol.44, p.2 (1988).

71. J. R. Park and D. D. Macdonald, Corrosion Sci Vol 23, 295 (1983).

72. R. DeLevie, Electrochimica Acta, Vol.9, p.1231 (1964).

73. Keiser, H., Beccu, K., and Gutjahr, M., Electrochim. Acta, Vol.21, p.539, 1976.

74. Feliu, S., Gonzalez, J., Andrade, C. and Feliu, V., Materials and Structures, Vol. 22, p.199, 1989.

75. Feliu, S., Gonzalez, J., Andrade, C. and Feliu, V., Corrosion Science, Vol. 29, p.105, 1989.

76. Feliu, S., Gonzalez, J., Andrade, C. and Feliu, V., Corrosion, Vol. 44, p.761, 1988.

77. Thompson, N., Lawson, K., and Beavers, J., Corrosion, Vol. 44, p.581, 1988.

78. Lemoine, L., Wenger, F. and Galland, J., "Study of the Corrosion of Concrete Reinforcement by Electrochemical Impedance Measurement", p. 118 in Corrosion Rates of Steel in Concrete, ASTM STP 1065, N. Berke, V. Chaker and D. Whiting, Eds., ASTM, Philadelphia, 1990.

79. Sluyters, J.H., Recueil, Vol. 79, p.1092, 1960.

80. Sluyters, J.H. and Oomen, J.J., Recueil, Vol. 79, p.1101, 1960.

81. John. D.G., Searson, P.C. and Dawson, J.L., Br. Corr. J., Vol 16, p.102, 1981.

82. Haruyama, S. and Tsuru, T., "A Corrosion Monitor Based on Impedance Method", p.167 in Electrochemical Corrosion Testing, ASTM STP 727, F. Mansfeld and U. Bertocci, Eds., ASTM, Philadelphia, 1981.

83. D. Macdonald, M. McKubre and M. Urquidi-Macdonald, Corrosion, Vol.44, p.2 (1988).

84. J. R. Park and D. D. Macdonald, Corrosion Sci Vol 23, 295 (1983).

85. Macdonald, D., Urquidi-Macdonald, M., and El-Tantawy, Y., Corrosion, Vol. 47, p. 330, 1991.

86. Kranc, S.C. and Sagüés, A.A., "Calculation of Extended Counter Electrode Polarization Effects on the Electrochemical Impedance Response of Steel in Concrete", in Electrochemical Impedance: Interpretation and Analysis, ASTM STP 1188, D.C. Silverman, J.R. Scully and M.W. Kendig, Eds., American Society for Testing and Materials, Philadelphia, 1993.

87. Oltra, R. and Keddam, M., Corrosion Sci. Vol. 28, p. 1 (1988).

88. Matsuoka, K., Kihira, H., Ito, S., and Murata, T., "Corrosion Monitoring for Reinforcing Bars in Concrete", p. 103 in Corrosion Rates of Steel in Concrete, ASTM STP 1065, N. Berke, V. Chaker and D. Whiting, Eds., ASTM, Philadelphia, 1990.

89. Feliu, S.,Gonzalez, J., Escudero, M.,and Andrade, C., "Influence of Counter Electrode Size on the On-Site Measurement of Polarization Resistance in Concrete Structures", Paper No. 142, Corrosion/90, National Association of Corrosion Engineers, Houston, 1990.

90. John, D., Eden, D., Dawson, J. and Langford, P., "Corrosion Measurements of Reinforcing Steel and Monitoring of Concrete Structures", Paper No. 136, Corrosion/87, National Association of Corrosion Engineers, Houston, 1987.

91. Kranc, S.C. and Sagüés, A., "Polarization Current Distribution and Electrochemical Impedance Response of Reinforced Concrete when Using Guard ring Electrodes", presented and submitted for publication in the proceedings of the 2nd. International Conference on Electrochemical Impedance Spectroscopy, Santa Barbara, California, July 12-17, 1992.

92. Zayed, A. and Sagüés, A., Corrosion Science Vol.30, p.1025, 1990.

93. Sagüés, A. and Zayed, A., Corrosion, Vol. 47, p.852, 1991.

94. Virmani, Y., Clear, K. and Pasko, T., Time to Corrosion of Reinforcing Steel in Concrete Slabs, Vol.5:Calcium Nitrite Admixture and Epoxy-Coated Reinforcing Bars as Corrosion Protection Systems, Report No. FHWA/RD-83/012, National Technical Information Service, Springfield, Virginia, 1983.

95. Scannel, T. and Clear, K., Long Term Outdoor Exposure Evaluation of Concrete Slabs Containing Epoxy Coated Reinforcing Steel, Transportation Rsch. Board , 69th Annual Meeting, Paper Preprint No. 89-0431, Washington, January 7-11, 1990.

96. Berke, N., Shen, D., and Sundberg, K., "Comparison of the Polarization Resistance Technique to the Macrocell Corrosion Technique", p. 38 in Corrosion Rates of Steel in Concrete, N. Berke, Ed., STP 1065, ASTM, Philadelphia, 1990.

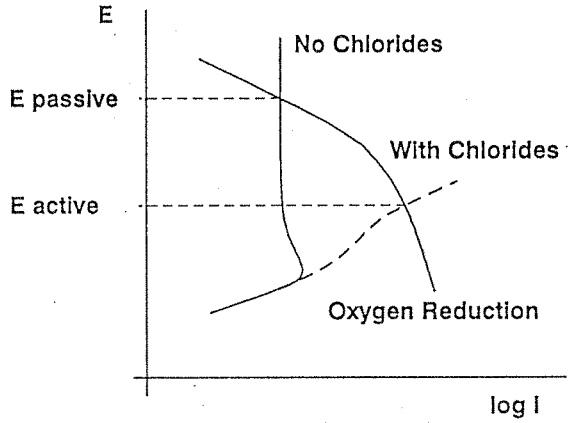

Figure 1. Potential shift due to chloride ion-induced depassivation.

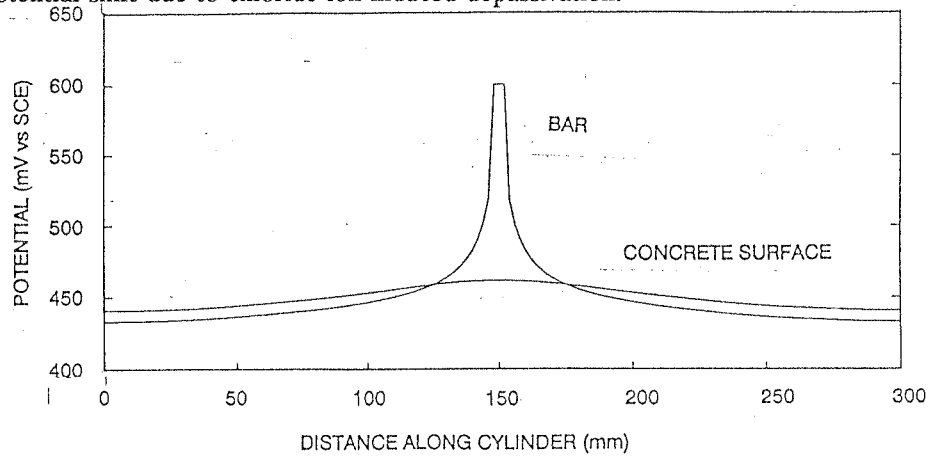

Figure 2. Computed potential distributions for an 11 cm diameter, 30 cm long concrete cylinder containing an axial 1 cm rebar. A 6 mm long ring-shaped region is active at the center of the rebar length, while the rest is passive. The potential distribution at the concrete next to the bar surface sharply varies with the corrosion condition of the steel. The potential at the external concrete surface shows much less variation (adapted from Ref.[38]).

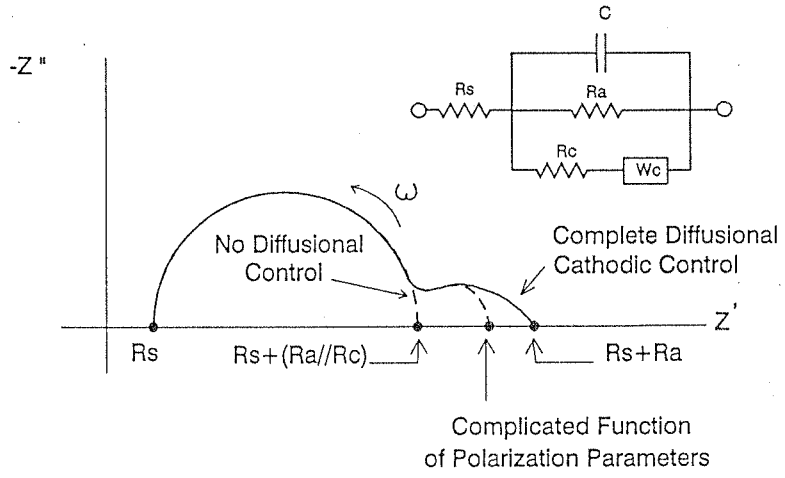

Figure 3. EIS response of a mixed-potential system. Ra and Rc rpresent the activation component of the anodic and cathodic impedances respectively. Wc is a diffusional impedance term for the cathodic reaction and C is the interfacial capacitance. Depending on the extent of diffusional control, the low-frequency limit of the impedance could vary between the values shown (// denotes parallel combination).

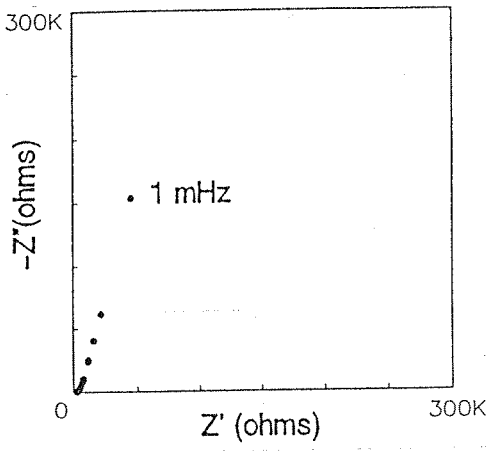

Figure 4. CPA behavior of sandblasted passive steel in concrete (from Ref.[63]. Rebar segment 5 cm long, 1 cm diameter in dry concrete.

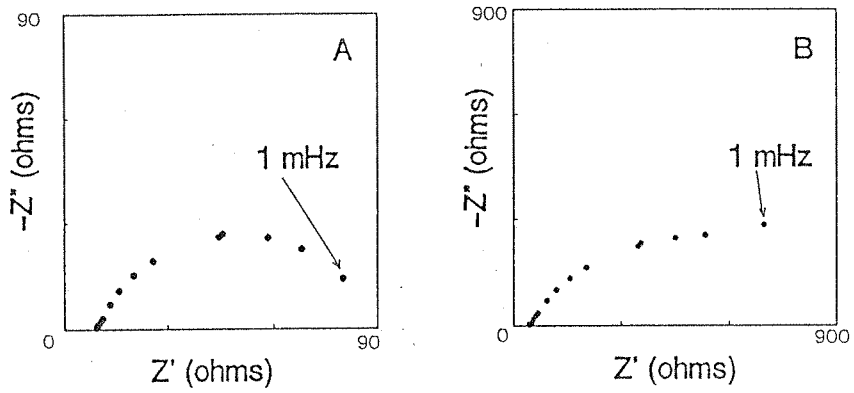

Figure 5 - Examples of typical EIS behavior of reinforced concrete beams undergoing active corrosion. In (A) the data tend to converge toward the real axis at the low frequency limit. In (B) the phase angle remains high at the lowest test frequencies.
A: 3 m-long beam, half of the length submerged in 15% NaCl solution.
B: 0.45 m-long column, lower 17.5 cm submerged in a 9000 ppm Cl^- solution [63].

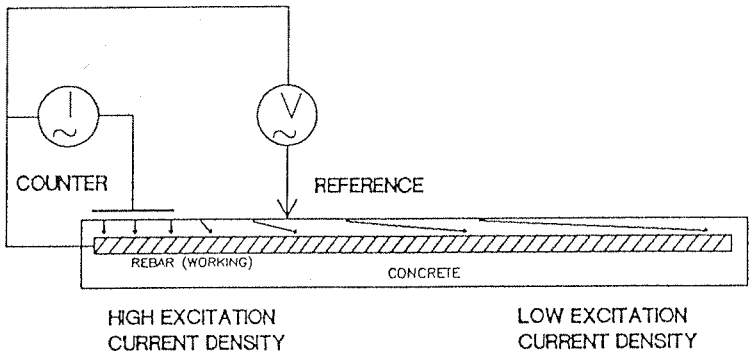

Figure 6 - Reinforced concrete beam excited near one end by an ac current source (I). Because of finite concrete conductivity, the excitation current density is highest near the counter electrode. Impedance calculations based on the measured ac voltage (V) and the excitation current will give different values along the beam.

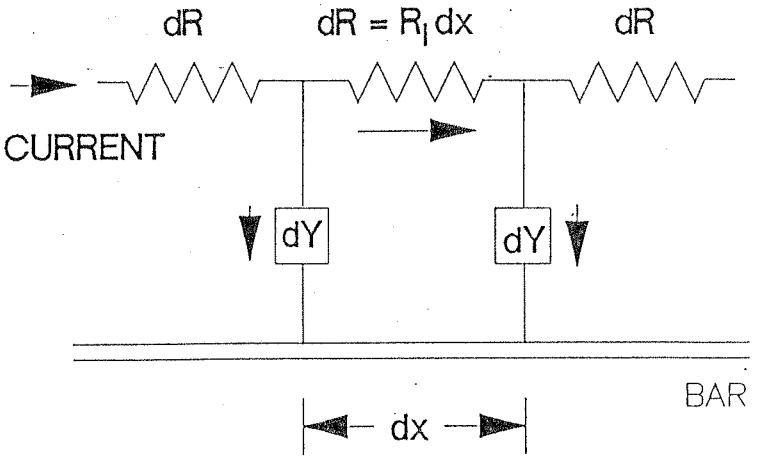

Figure 7 - Transmission-line model of a slender reinforced concrete beam.

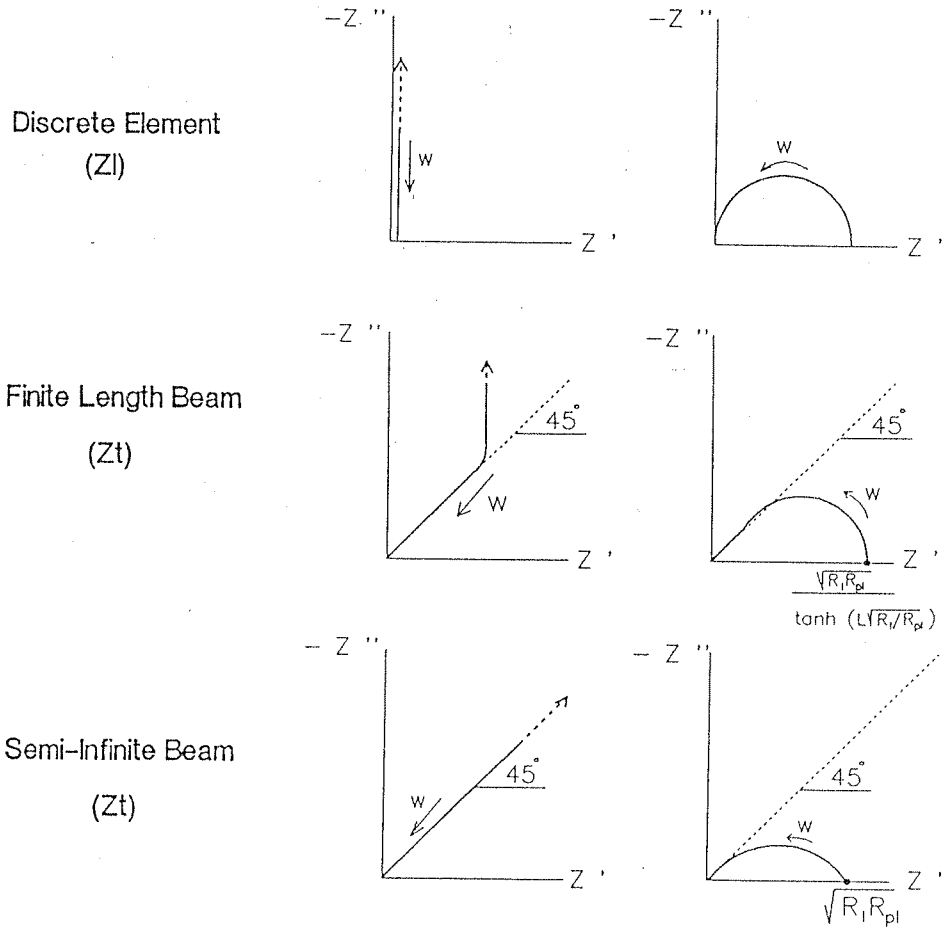

Figure 8. Impedance behavior expected for a discrete electrode (top diagram) and based on Eqs. (4) and (5) for a slender reinforced concrete beam excited at one end (center and bottom diagrams). The left side diagrams show the response in the absence of corrosion. The right side shows the response under uniform corrosion conditions, assuming that the impedance of each surface element corresponds to a simple polarization resistance-interfacial capacitance combination.

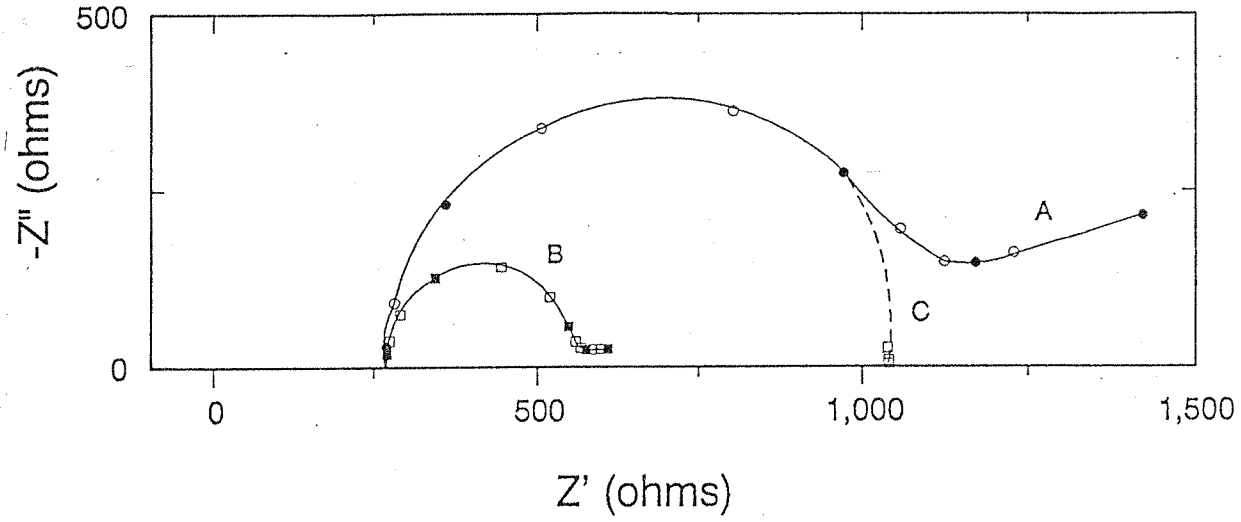

Figure 9. Calculated EIS response for the system in Figure 1. Curve A: considering both diffusional impedance and current distribution effects; Curve C: same as (A) but assuming that the impedance is determined only by activation terms; Curve B: EIS response that would have been obtained if the concrete resistance were negligible but the corrosion distribution were the same as in (A). The origin of curve (B) was shifted to facilitate comparison. Adapted from Ref.[38].

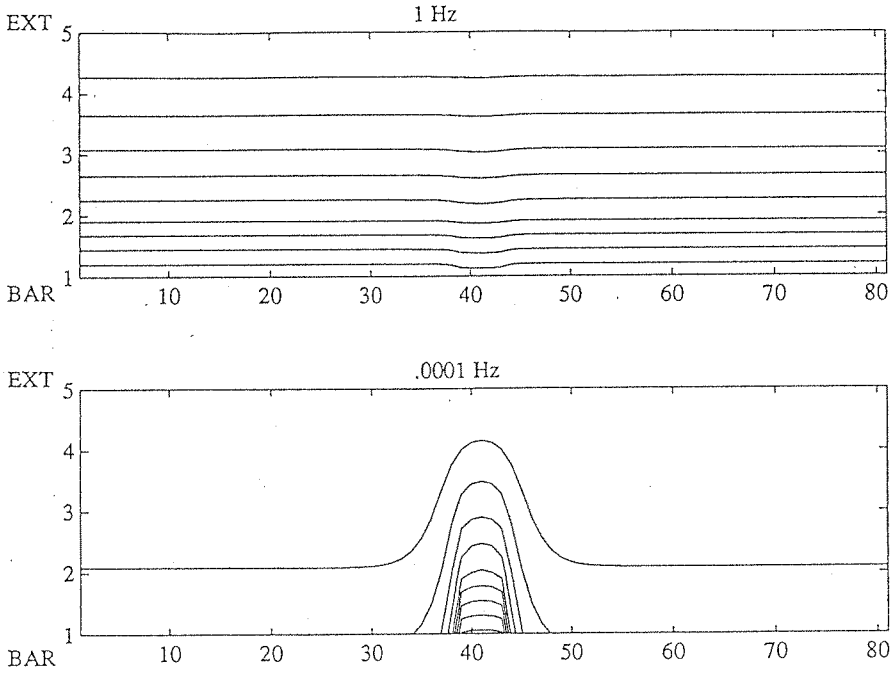

Figure 10. A.C. potential distribution at two extreme frequencies for a reinforced concrete cylinder with an external, wrap-around counter electrode. A small active region is present at the center of the axial rebar. The diagram shows equipotential (effective voltage) lines placed at 1 mV intervals in the longitudinal cross section of the cylinder. Potential at the external surface (top) was 10 mV; the bar (bottom) was ground. The numbers correspond to computational nodes. The actual aspect ratio of the cross section is 27 (length) to 1 (height). From Ref. [86].